

Development of n-in-p pixel modules for the ATLAS Upgrade at HL-LHC

A. Macchiolo, R. Nisius, N. Savic, S. Terzo

Max-Planck-Institut für Physik, Föhringer Ring 6, D-80805 Munich, Germany

Abstract

Thin planar pixel modules are promising candidates to instrument the inner layers of the new ATLAS pixel detector for HL-LHC, thanks to the reduced contribution to the material budget and their high charge collection efficiency after irradiation. 100-200 μm thick sensors, interconnected to FE-I4 read-out chips, have been characterized with radioactive sources and beam tests at the CERN-SPS and DESY. The results of these measurements are reported for devices before and after irradiation up to a fluence of $14 \times 10^{15} \text{ n}_{\text{eq}}/\text{cm}^2$. The charge collection and tracking efficiency of the different sensor thicknesses are compared. The outlook for future planar pixel sensor production is discussed, with a focus on sensor design with the pixel pitches (50×50 and $25 \times 100 \mu\text{m}^2$) foreseen for the RD53 Collaboration read-out chip in 65 nm CMOS technology. An optimization of the biasing structures in the pixel cells is required to avoid the hit efficiency loss presently observed in the punch-through region after irradiation. For this purpose the performance of different layouts have been compared in FE-I4 compatible sensors at various fluence levels by using beam test data. Highly segmented sensors will represent a challenge for the tracking in the forward region of the pixel system at HL-LHC. In order to reproduce the performance of $50 \times 50 \mu\text{m}^2$ pixels at high pseudo-rapidity values, FE-I4 compatible planar pixel sensors have been studied before and after irradiation in beam tests at high incidence angle (80°) with respect to the short pixel direction. Results on cluster shapes, charge collection and hit efficiency will be shown.

Keywords: Pixel detector, n-in-p, ATLAS, HL-LHC

1. Introduction

In this paper, different designs of n-in-p planar hybrid pixel modules are investigated and compared. The R&D activity is carried out in view of the upgrade of the ATLAS pixel system for the High Luminosity phase of the LHC (HL-LHC) [1], foreseen to start around 2025. The number of pile-up events per bunch crossing expected at the HL-LHC is 140-200 [2, 3]. To keep the pixel occupancy at an acceptable level, smaller pixel cell dimensions are foreseen with respect to the ones presently implemented in the FE-I3 chip ($50 \mu\text{m} \times 400 \mu\text{m}$) and in the FE-I4 chip ($50 \mu\text{m} \times 250 \mu\text{m}$), developed for the ATLAS Insertable B-Layer (IBL) [4]. The new readout chips for the ATLAS and CMS pixel systems at HL-LHC are being developed by the CERN RD53 Collaboration [5] with a pitch of $50 \mu\text{m} \times 50 \mu\text{m}$ in the 65 nm CMOS technology. The feasibility of employing thin planar pixel detectors for the inner layers of the upgraded ATLAS pixel system is being investigated, comparing the performance of sensors in the thickness range of 100-200 μm . Using the SOI technology, n-in-p sensors with a full thickness of 100 and 200 μm were produced on 6" wafers at VTT in the framework of a Multi-project Wafer run (MPW) [6].

This production also implements activated edges to reduce the inactive area of these devices [7] [8] and the performance in terms of charge collection at the edges has been presented elsewhere [9]. 200 μm thick sensors were also produced at CIS, on 4" wafers, with a standard guard ring structure and an inactive width of 450 μm [10].

The sensors have been interconnected by bump-bonding to

FE-I4 chips and characterized by means of radioactive sources in the laboratory and beam test experiment with 4 GeV electrons at DESY and 120 GeV pions at CERN-SPS.

2. Characterization of sensors with different thickness after irradiation

The charge collection properties were measured by means of Strontium source scans using the ATLAS USBpix read-out system, developed by the University of Bonn [11]. The pixel modules were investigated before and after irradiation, up to a fluence of $5 \times 10^{15} \text{ n}_{\text{eq}}/\text{cm}^2$ for the 100 μm thick sensors, corresponding to the integrated fluence at the end of the life-time for the second pixel layer at HL-LHC and for the 200 μm thick sensors up to a fluence of $14 \times 10^{15} \text{ n}_{\text{eq}}/\text{cm}^2$, the expected value for the inner layer after ten years of operation at HL-LHC. Fig.1 shows the collected charge for the 100 μm thick sensors, as a function of the applied bias voltage for different fluences. It can be observed that the collected charge starts to saturate at moderate bias voltages, between 200 and 300V, in the full fluence range explored, to values that are very close to those expected for not irradiated detectors, around 6500-7000 electrons [12]. Fig.2 shows the results of the charge collection for the 200 μm thick sensors and of 300 μm thick sensors at the highest fluence only. After $2 \times 10^{15} \text{ n}_{\text{eq}}/\text{cm}^2$, no saturation of the charge is observed. At the maximum fluence of $14 \times 10^{15} \text{ n}_{\text{eq}}/\text{cm}^2$, the collected charge of the 200 and 300 μm thick sensors becomes very similar and at the highest measured voltage of 1000V is between 5 ke and 5.5 ke.

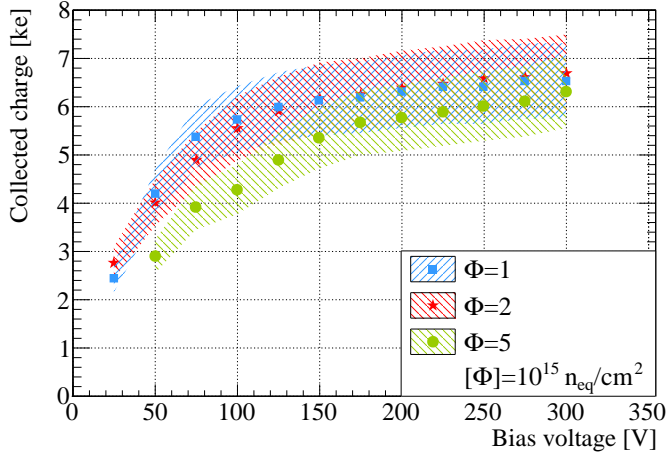


Figure 1: Charge collection of 100 μm thick sensors as a function of the bias voltage for different fluences

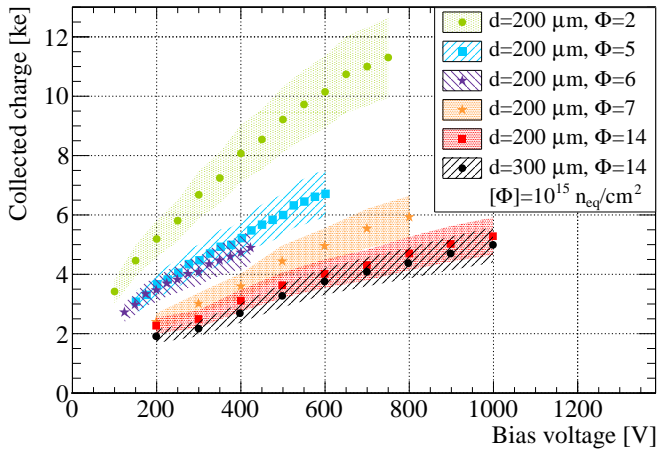


Figure 2: Charge collection of 200 and 300 μm thick sensors as a function of the bias voltage for different fluences

FE-I3 and FE-I4 modules of different thickness were also investigated in beam tests by using telescopes of the EUDET family [13]. The irradiated modules were cooled with dry ice inside a box designed on purpose. With this setup typical temperatures between -50°C and -40°C are obtained during operations. Recent studies have shown the independence of the collected charge in a temperature range between -50°C and -25°C [14] and between -50°C and -40°C for the hit efficiency [15]. Figure 3 summarizes the results of the hit efficiency in a fluence range between 4 and $6 \times 10^{15} \text{ n}_{\text{eq}}/\text{cm}^2$. The 150 μm thick sensors were obtained from an older production at MPG-HLL on SOI 6" wafers while the 285 μm thick sensors were produced on 4" wafers at CIS, as described in more details in [12]. For all the values of the hit efficiencies quoted in the following, the dominant source of uncertainty is systematic and evaluated to be 0.3%, as explained in [16]. After an irradiation fluence between 4 and $6 \times 10^{15} \text{ n}_{\text{eq}}/\text{cm}^2$, FE-I4 modules with 150 and 200 μm thick sensors show similar performances reaching a hit efficiency of about 97% at $V_{\text{bias}}=500\text{V}$, while the same module type with a 100 μm thick sensor starts to saturate to this value

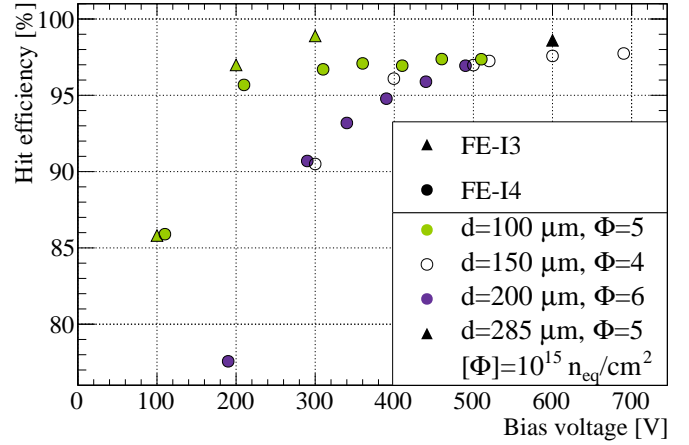


Figure 3: Hit efficiency as a function of the bias voltage for pixel modules of different thicknesses irradiated to a fluence between 4 and $6 \times 10^{15} \text{ n}_{\text{eq}}/\text{cm}^2$. The modules were operated at a threshold of 1600 e.

of the hit efficiency already at a bias voltage of 300V. These results suggest that a lower operational bias voltage is possible for thinner sensors, and a reduced power dissipation at these fluence levels. Fig.4 shows the expected sensor power density for these devices at a temperature of -25°C , at which it is foreseen that the sensors will be operated at HL-LHC, as a function of the applied bias voltage for different values of the sensor thickness. A high power consumption requires sufficient performance of the cooling system to dissipate the heat and avoid the thermal runaway of the sensor. Since this effect limits the achievable operational voltage of the modules, it has to be considered together with the hit efficiency results to determine the practical performance of the different sensor thicknesses. The power per area calculated for the thinner sensors of 100 and 150 μm at the optimal operational voltage of 300 and 500V estimated from the hit efficiency measurements in Fig.3, is respectively 8 and 3.5 times lower than the runaway point of the worst case considered. The runaway point was calculated with the parameters described in [10], except for the higher chip power dissipation of $0.74 \text{ W}/\text{cm}^2$ assumed for the RD53 Collaboration read-out chip in 65 nm CMOS technology.

3. Optimization of the pixel cell design

Figure 3 shows that at equal fluence and thickness, FE-I3 modules yield a hit efficiency 1% higher with respect to the FE-I4. This is due to the lower fraction of area that the biasing structures occupy in the pixel cell, since the punch-through dot and the bias rail are implemented with the same design and the FE-I3 pixel length is 400 μm compared with the 250 μm in the FE-I4 case. It has found that these elements induce a decrease of the hit efficiency in the pixel cell [10]. Given the reduced pitch for the future pixel read-out chips, an optimization of the biasing structures is mandatory, to avoid a large loss of hit efficiency after irradiation, especially in the central pseudo-rapidity region.

Different designs of the bias dot and rail were thus implemented

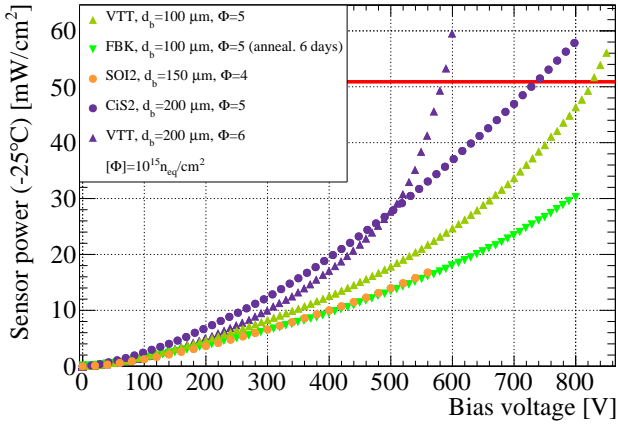


Figure 4: Power density as a function of the bias voltage for sensors irradiated between 4 and 6×10^{15} n_{eq}/cm^2 estimated at a temperature of $T=-25$ °C. The horizontal red line indicates the thermal runaway point as calculated in [10].

in two different pixel sensors, both compatible with the FE-I4 chip, of a recent n-in-p production carried out at CIS on 6" wafers, with a thickness of $270 \mu m$. The first one includes three designs, repeated in every successive group of 30 rows, with a single bias dot for every pixel: the standard design (Fig. 5 (a)) with the rail at the center between the short side of two neighbouring pixels, a slightly modified version with the rail running over the bias dot (b) and the last one (c), with the rail over the central part of the cell. After irradiation at a fluence of 3×10^{15} n_{eq}/cm^2 , the hit efficiencies of the different designs have been compared. The highest value of 98.7% has been found for the geometry (b), while the standard geometry yields an efficiency of 97.7%. The layout in Fig. 5 (c) shows the lowest efficiency, especially in correspondence of the horizontal lines of the bias rail that runs in the inter-pixel region. It can instead be observed that where the bias rail is superimposed to the pixel implant, both in (b) and in (c), the aluminum line does not induce any efficiency loss because the effects on the electric field shapes are then screened by the pixel implant.

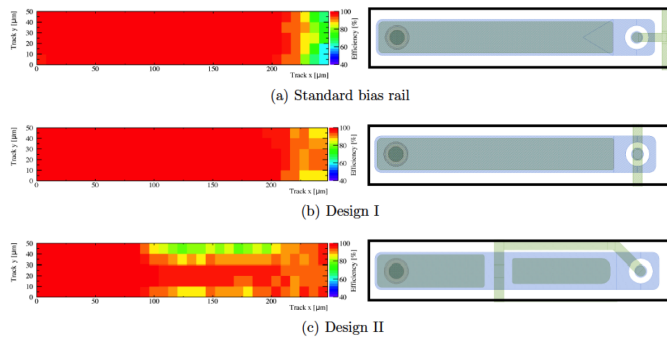


Figure 5: Hit efficiency projected onto a pixel cell for different single bias dot designs after an irradiation fluence of 3×10^{15} n_{eq}/cm^2 . The module was operated at 800V.

Higher hit efficiencies are obtained by implementing an external punch-through dot, common to four pixels, as shown by Fig. 6 and 7. In this case the sensor pitch is $25 \mu m \times 500 \mu m$,

still compatible with a FE-I4 chip. The overall area where a lower hit efficiency is observed is clearly reduced with respect to the standard FE-I4 design. The hit efficiency reaches 99.4% at the highest measured voltage of 500V which is around 2% higher than the 97.7% measured for the standard FE-I4 design at the same fluence.



Figure 6: Layout of the $25 \times 500 \mu m^2$ FE-I4 compatible sensor design with an external punch-through common to four pixel cells. The insert is a photograph of the produced device superimposed to the schematic design of the sensor.

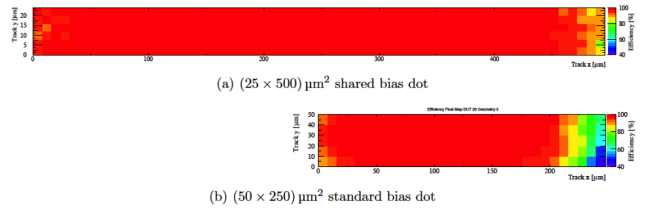


Figure 7: Comparison of the hit efficiency over the pixel cell for the FE-I4 modules of the CIS3 production irradiated to a fluence of 3×10^{15} n_{eq}/cm^2 with different bias structures. (a) shows the hit efficiency for the module with $25 \times 500 \mu m^2$ pitch and one common bias dot shared among four pixels. (b) shows the hit efficiency for the standard FE-I4 design with an internal punch-through dot and a pitch of $50 \times 250 \mu m^2$.

Two new pixel sensor productions at ADVACAM and CIS, with 100 and 150 μm thickness, have recently been completed and they include FE-I4 compatible devices with $50 \mu m \times 250 \mu m$ pitch and the new external punch-through biasing structures. It is planned to repeat the hit efficiency measurements with these sensors in a fluence range up to 10^{16} n_{eq}/cm^2 to confirm the better performance observed with the new biasing design with thinner devices.

4. Performance of n-in-p planar pixels at high ϕ

The smaller pixel cell dimensions foreseen at HL-LHC pose a severe challenge also for the tracking in high pseudo-rapidity regions (high η) of the new trackers. To investigate the hit efficiency for a cell size of $50 \mu m \times 50 \mu m$ at $\eta=2.5$, FE-I4 modules were investigated with an electron beam at DESY crossing the sensor with an angle of $\phi=80^\circ$ with respect to the pixel surface. In this set-up the particles cross the pixel cells along the $50 \mu m$ side, allowing to study the performance of a $50 \mu m \times 50 \mu m$ sensor at high η . Figure 8 shows how the cluster size along η is strongly dependent on the sensor thickness, with thinner sensors yielding the smaller clusters and resulting in the lower pixel occupancy. The first module employed in this test is a not irradiated device, 100 μm thick, from the VTT production. Track

reconstruction was not possible for the data sample recorded, and the analysis was performed using the hit information of the long clusters corresponding to a single particle traversing the sensor. The cluster size and hit efficiency were calculated under varying assumptions on the allowed number of holes in the cluster (defined as cluster distance). Given the fact that the particle path in silicon is only around $50 \mu\text{m}$ long, with an expected most probable value (MPV) of the collected charge of 3100 e, a dedicated tuning was performed, with a low target threshold of 1000 e. Fig.9 shows the single hit inefficiency as a function of the maximum value of the distance between two pixels allowed while building a cluster (cluster separation). The single hit inefficiency is defined as the number of holes (h^c_{miss}) divided by the cluster length w_x^c , not including the entrance and exit pixels, since these are 100% efficient by definition. It can be observed that values of the hit efficiency close to 100% are obtained with this thin sensor module, for all the cluster distance hypothesis, suggesting the feasibility of employing this kind of detectors at high η values at HL-LHC.

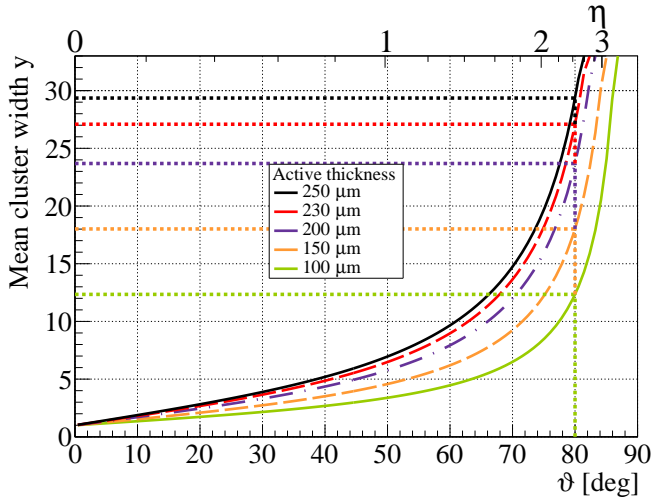


Figure 8: Mean cluster width along the short pixel cell side for a FE-I4 module placed at high ϕ in the beam, as a function of beam incidence angle. The relationship is also valid for a pixel sensor with $50 \mu\text{m} \times 50 \mu\text{m}$ pitch at high η with respect to the beam.

A similar analysis was performed with a module assembled with a $200 \mu\text{m}$ thick sensor and irradiated to a fluence of $2 \times 10^{15} \text{ n}_{\text{eq}}/\text{cm}^2$. The charge distribution in the depth of the silicon bulk is shown in Fig.10, for a bias voltage range between 300 and 800V, in the case of cluster size equal to 24 where, according to Fig.8 the particle crosses all the depth of the sensor. Pixel number 0 corresponds to the front side and pixel 24 to the backside of the sensor. It can be observed that for lower bias voltages the collected charge decreases in the backside while at a bias voltage of 800V, resulting in a higher electric field throughout the bulk of the sensor, the charge collection is more uniform. The hit efficiency for the single pixels of this irradiated module is shown in Fig.11, also in this case only for a cluster size of 24. At a bias voltage of 800V, the range of the hit efficiency is (81.5-93.4)% at the different depths.

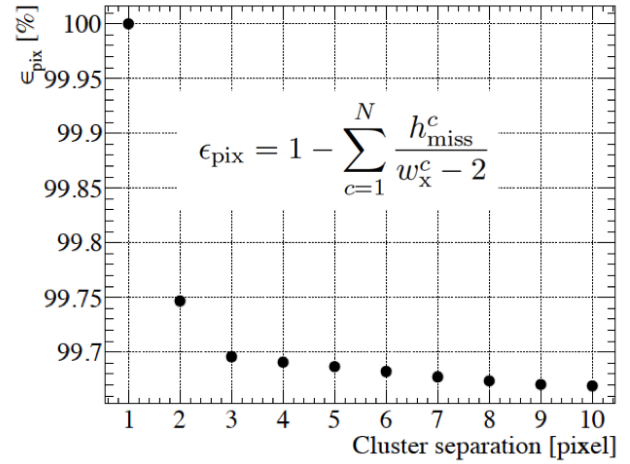


Figure 9: Hit efficiency of single pixels as a function of the cluster separation for an FE-I4 module employing a $100 \mu\text{m}$ thick sensor and tilted by 80° around its x axis with respect to the perpendicular beam incidence. The single hit inefficiency is defined as the number of holes (h^c_{miss}) divided by the cluster length w_x^c , not including the entrance and exit pixels, since these are 100% efficient by definition. The sum is over all the N reconstructed clusters for a given choice of the cluster separation value.

5. Conclusions

Pixel modules assembled with thin planar sensors were investigated for the upgrade of the ATLAS pixel system at HL-LHC. Charge collection properties and hit efficiency were analysed after irradiation for sensor thicknesses in the range from 100 to $200 \mu\text{m}$. For integrated radiation fluences of $(4-6) \times 10^{15} \text{ n}_{\text{eq}}/\text{cm}^2$, as expected for the second pixel layer at HL-LHC, the best performance was observed for $100 \mu\text{m}$ thick sensors which reach the same hit efficiency as thicker sensors already with a bias voltage of 200-300V. The highest hit efficiency obtained for perpendicular incident tracks at these fluences is around (97-98)%, with the main inefficiency regions corresponding to the bias dot and the bias rail areas of the pixel cell. New biasing structures with an external bias dot common to four pixel cells have been investigated for thicker sensors and found to yield an higher hit efficiency, when compared to the standard design. It is now planned to study the performance of this new layout when implemented in 100 and $150 \mu\text{m}$ thin sensors.

Studies of cluster properties were performed for the pixel modules in the innermost layer at high pseudorapidity for the new pixel system at HL-LHC, where the particles traverse several pixels. In these conditions, thinner sensors have the advantage of a lower cluster size which results in a reduced occupancy and, after irradiation, are expected to perform better since the higher electric field counteracts trapping. For the ATLAS Phase II detector a smaller pitch in the z direction is foreseen, which together with an optimal single pixel efficiency would allow to increase the precision for measuring the entrance and the exit point of particles crossing the pixel modules at high pseudorapidity and thus obtaining a track seed with the standalone innermost layer [17]. The performance of a $50 \mu\text{m}$ pitch along z was therefore investigated with FE-I4 modules placed at high ϕ angle with respect to the beam direction, showing a single

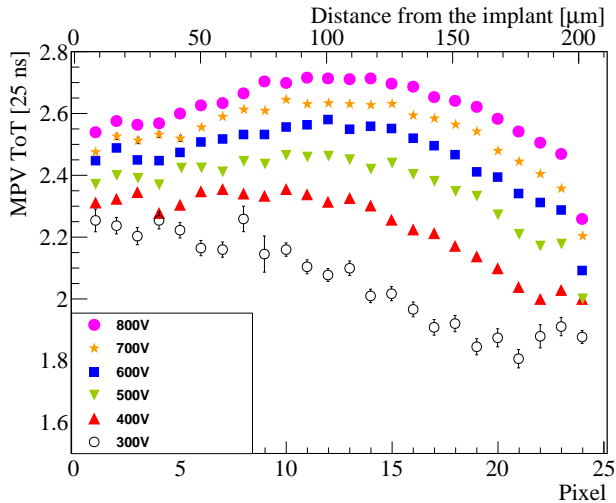


Figure 10: Charge collection, expressed in units of Time over Threshold, as a function of the pixel number for a value of the cluster size equal to 24, obtained with a FE-I4 module, irradiated to a fluence of $2 \times 10^{15} \text{ n}_{\text{eq}}/\text{cm}^2$, employing a $200 \mu\text{m}$ thick sensor and tilted by 80° around its x axis with respect to the perpendicular beam incidence. The pixel number equal to 0 corresponds to the front side and 24 to the backside of the sensor.

pixel efficiency more than 99.6% before irradiation for $100 \mu\text{m}$ thin sensors. A hit efficiency of (81.5-93.4)% was instead reconstructed for a module with a $200 \mu\text{m}$ thin sensor irradiated at a fluence of $2 \times 10^{15} \text{ n}_{\text{eq}}/\text{cm}^2$. These measurements after irradiation will be also continued with thinner sensors in a wider fluence range.

6. Acknowledgements

This work has been partially performed in the framework of the CERN RD50 Collaboration. The authors thank V. Cindro for the irradiation at JSI and A. Dierlamm for the irradiation at KIT. Supported by the H2020 project AIDA-2020, GA no. 654168. <http://aida2020.web.cern.ch/>

References

- [1] O. Brüning, L. Rossi, et al., "High-Luminosity Large Hadron Collider; A description for the European Strategy Preparatory Group", Tech. Rep. CERN-ATS-2012-236, CERN (Geneva, 2012).
- [2] HL-LHC Parameter and Lay-out Committee, HL-LHC Parameters V4.1.1, (Last updated on 16 December 2014), <https://espace.cern.ch/HiLumi/PLC/default.aspx>.
- [3] O. Brüning and F. Zimmermann, Parameter Space for the LHC Luminosity Upgrade, Proceedings of the 3rd International Conference on Particle Accelerator (IPAC 2012) (2012) 127.
- [4] M. Capeans et al., ATLAS Insertable B-Layer Technical Design Report, CERN-LHCC-2010-013, Geneva Sep. 2010.
- [5] <http://rd53.web.cern.ch/RD53/>
- [6] J. Kalliopuska et al., "Processing and characterization of edgeless radiation detectors for large area detection", Nucl. Instr. and Meth. A 731 (2013) 205-209. doi:10.1016/j.nima.2013.06.097
- [7] S. Eranen et al., "3D processing on 6 in. high resistive SOI wafers: Fabrication of edgeless strip and pixel detectors", Nucl. Instr. and Meth. A607 (2009) 85.
- [8] X Wu et al., "Recent advances in processing and characterization of edgeless detectors", JINST 7 (2012), <http://dx.doi.org/10.1088/1748-0221/7/02/C02001>.

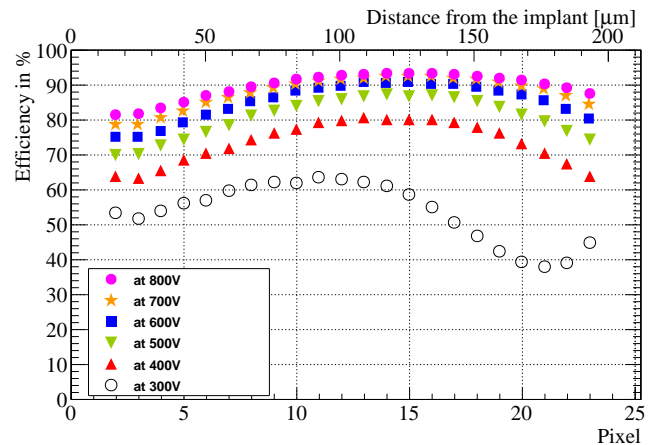


Figure 11: Hit efficiency as a function of the pixel number for a value of the cluster size equal to 24, module employing a $200 \mu\text{m}$ thick sensor and tilted by 80° around its x axis with respect to the perpendicular beam incidence. The x axis on the top indicates the corresponding value of the depth in the silicon bulk with 0 being the frontside and $200 \mu\text{m}$ the backside. The efficiencies of the first and the last pixels are by construction 100% since they define the cluster length.

- [9] S. Terzo et al., "Heavily irradiated n-in-p thin planar pixel sensors with and without active edges", Proceedings of the iWoRID 2013 Conference, JINST 9 (2014) C05023.
- [10] S. Terzo, "Development of radiation hard pixel modules employing planar n-in-p silicon sensors with active edges for the ATLAS detector at HL-LHC", Ph.D. thesis, TU Munich, 2015.
- [11] <http://icwiki.physik.uni-bonn.de/twiki/bin/view/Systems/UsbPix#Hardware>
- [12] P. Weigell, "Investigation of Properties of Novel Silicon Pixel Assemblies Employing Thin n-in-p Sensors and 3D-Integration", PhD Thesis, (2013), TU Muenchen CERN-THESIS-2012-229.
- [13] I. Rubinskiy, "An EUDET/AIDA Pixel Beam Telescope for Detector Development", Phys. Proc. 37 (2012) 923.
- [14] N. Savic et al., "Investigation of hit efficiency of n-in-p pixels with different designs", presented at the 26th RD50 Workshop, Santander, <https://indico.cern.ch/event/381195/>.
- [15] N. Savic et al., "Thin n-in-p planar pixel sensor productions at MPP", presented at the 27th RD50 Workshop, CERN, (2015), <https://indico.cern.ch/event/456679/>.
- [16] J. Weingarten, et al., "Planar Pixel Sensors for the ATLAS Upgrade: Beam Tests results", accepted by JINST, <http://arxiv.org/abs/arXiv:1204.1266>.
- [17] S. Viel et al., "Performance of Silicon Pixel Detectors at Small Track Incidence Angles for the ATLAS Inner Tracker Upgrade", ATL-INDET-PROC-2015-011, <https://cds.cern.ch/record/2065104/files/ATL-INDET-PROC-2015-011.pdf>